ACS APPLIED MATERIALS & INTERFACES

Research Article

www.acsami.org

Single-Step and Rapid Growth of Silver Nanoshells as SERS-Active Nanostructures for Label-Free Detection of Pesticides

Jin-Kyoung Yang,[†] Homan Kang,[‡,#] Hyunmi Lee,[†] Ahla Jo,[§] Sinyoung Jeong,[∥] Su-Ji Jeon,[⊥] Hye-In Kim,[⊥] Ho-Young Lee,[§] Dae Hong Jeong,[‡,∥] Jong-Ho Kim,*[,⊥] and Yoon-Sik Lee*[,†,‡]

[†]School of Chemical and Biological Engineering, Seoul National University, Seoul, 151-742, Republic of Korea

[‡]Interdisciplinary Program in Nano-Science and Technology, Seoul National University, Seoul, 151-742, Republic of Korea

[§]Department of Nuclear Medicine, Seoul National University Bundang Hospital, Seongnam, 463-707, Republic of Korea

[∥]Department of Chemistry Education, Seoul National University, Seoul, 151-742, Republic of Korea

[⊥]Department of Chemical Engineering, Hanyang University, Ansan, 426-791, Republic of Korea

Supporting Information

ABSTRACT: We explored a single-step approach for the rapid growth of Ag nanoshells (Ag NSs) under mild conditions. Without predeposition of seed metals, a uniform and complete layer of Ag shells was rapidly formed on silica core particles within 2 min at 25 °C via single electron transfer from octylamine to Ag^+ ions. The size and thickness of the Ag NSs were effectively tuned by adjusting the concentration of silica nanoparticles (silica NPs) with optimal concentrations of $AgNO_3$ and octylamine. This unusually rapid growth of Ag NSs was attributed to a significant increase in the reduction potential of the Ag^+ ions in ethylene glycol (EG) through the formation of an Ag/EG complex, which in turn led to their facile reduction by octylamine, even at room temperature. A substantial enhancement in the surface-enhanced Raman scattering (SERS) of the prepared Ag NSs was demonstrated. The Ag NSs were also utilized as SERS-active nanostructures for label-free detection of the pesticide thiram. The Ag NS-based SERS approach successfully detected thiram on apple peel down to the level of 38 ng/cm^2 in a label-free manner, which is very promising with respect to its potential use for the on-site detection of residual pesticides.

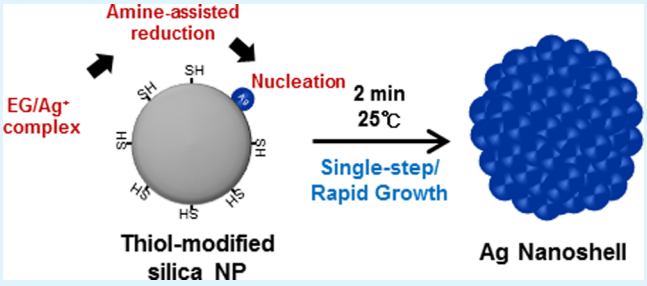

KEYWORDS: *silver nanoshells, seedless single-step synthesis, surface-enhanced Raman scattering, label-free pesticide detection*

INTRODUCTION

Metal nanoshells (NSs), which consist of a dielectric core coated with a metallic shell, have gained much attention in the fields of catalysis,[1] sensors,[2] drug delivery,[3] photothermal therapy,[4] surface-enhanced infrared absorption (SEIRA),[5] and surface-enhanced Raman scattering[6] because of their unique electronic and optical properties.[7,8] Plasmon resonance of novel metal NSs, such as Au and Ag NSs, can be effectively tuned to a desired wavelength ranging from the visible to the infrared region by varying the ratio of core size to metallic shell thickness.[9,10] Indeed, compared to nanospheres of Au and Ag, the plasmon resonance of Au and Ag NSs are much more controllable to obtain a wider range of optical spectra.[11,12]

Solid silver has been reported to have a stronger and sharper plasmon resonance than that of solid gold.[12,13] Consequently, the plasmon resonance of Ag NSs is also slightly stronger than that of Au NSs.[12] Solid silver exhibits much stronger Raman enhancement than solid gold, which is beneficial for sensitive detection of target molecules.[14,15] Ag NSs have been synthesized by several methods such as seed-mediated growth,[8,9,16−19] multistep layer-by-layer (LBL) deposition,[20−22] thermal evaporative methods,[23] and sonochemical processes.[24]

The most promising method for the uniform and complete formation of Ag NSs appear to be seed-mediated growth[8] and multistep LBL deposition.[20] However, the seed-mediated growth method requires additional presynthetic steps for the synthesis and deposition of seed metals, such as Au, Pd, or Sn, on the surface of core particles before subsequent growth of Ag shells at relatively high temperature (80 °C). In addition, the use of different seed metals can diminish the plasmon resonance of Ag NSs.[9] Several attempts have been made to synthesize Ag NSs without the predeposition of seed metals on a dielectric core,[25−29] but results have been unsatisfactory failing to produce a uniform and complete layer of Ag shells on the core surfaces. The LBL method produces Ag NSs more readily by stacking Ag NPs on core surfaces via electrostatic interaction. Nevertheless, this method is often a time-consuming process caused by the multistep deposition as well as the difficulty in producing a complete layer of Ag NSs because of the repulsion between particles. Hence, it is

Received: April 22, 2014
Accepted: July 2, 2014
Published: July 2, 2014

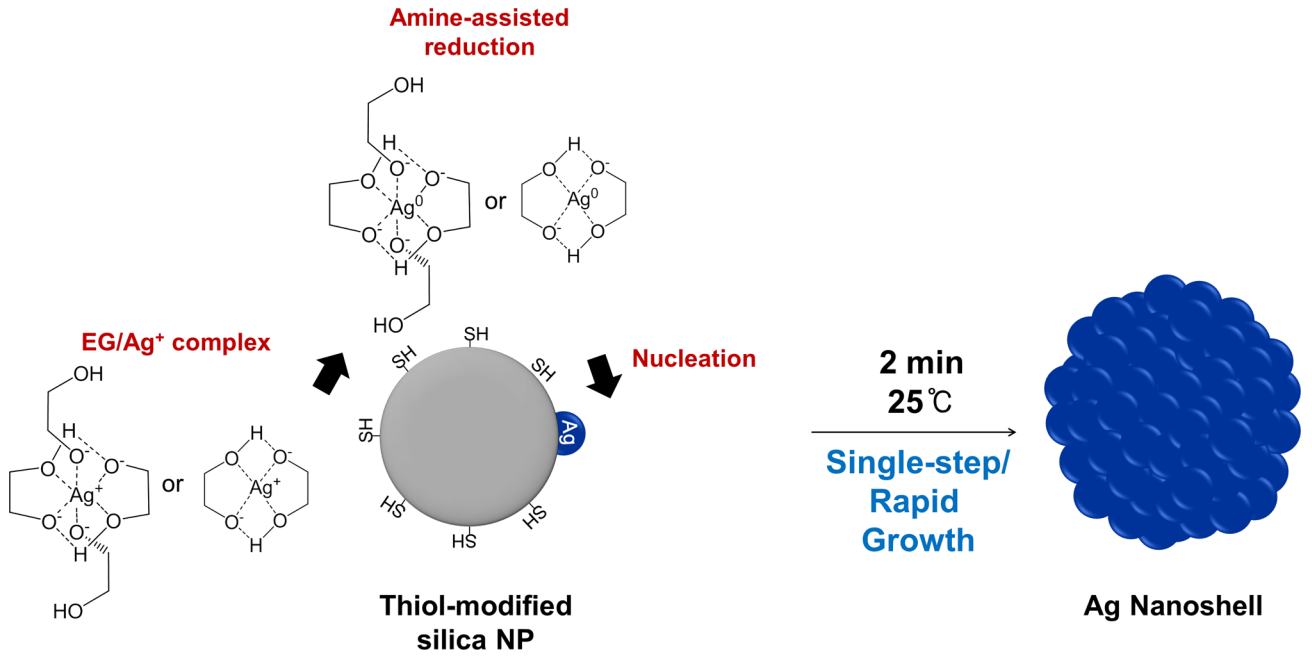

Figure 1. Schematic illustration for the fast single-step growth of Ag nanoshells (Ag NSs).

important to develop an effective, single-step strategy for the synthesis of a uniform and complete layer of Ag shell onto a dielectric core with a tunable plasmon resonance. Generating Ag NSs without the use of seed metals has remained a challenge.

Surface-enhanced Raman scattering (SERS) has been widely used as an analytical tool[30−33] for the sensitive detection of biomolecules,[34−36] pollutants,[37] and pesticides.[38−43] Among these applications, SERS-based detection of the pesticide,[38−43] bis(dimethylthio-carbamyl)disulfide, also known as thiram which prevents fungal diseases in seeds and crops,[44] has demonstrated more efficient and sensitive label-free detection compared to other methods such as chromatography,[45−47] colorimetry,[48] polarography,[49] and electrophoresis.[50] For SERS-based detection of thiram, the SERS-active nanostructures must be capable of inducing a strong electromagnetic (EM) field enhancement. Thus, Ag NSs should have appropriate properties as a SERS-active nanostructure for the label-free and sensitive detection of thiram.

Recently, we reported NIR-SERS probes based on Ag NSs prepared by an amine-assisted reduction method for cell-tracking in vivo.[51] However, comprehensive study to understand the mechanism responsible for the formation of Ag NSs under mild conditions was not undertaken. Herein, we present a systematic study of a seedless single-step method for the rapid growth of Ag NSs in the presence of octylamine as a mild reducing agent at room temperature. We found that a complete layer of Ag shells was quite rapidly formed onto silica nanoparticles (Si NPs) within 2 min. Thickness of Ag NSs was effectively controlled by varying the concentration of Si NPs, which resulted in a shift of plasmon resonance from the visible to the near-infrared (NIR) region. This rapid growth of Ag NSs was attributed to a significant increase in the reduction potential of the Ag^+ ions in ethylene glycol, which led to the facile reduction of the ions by octylamine even at room temperature. Finally, the Ag NSs produced were used as SERS-active nanostructures for the label-free detection of thiram. Through strongly enhanced Raman signals on the Ag NSs SERS substrate, thiram was effectively detected on apple peels at concentrations as low as 38 ng/cm^2. The Ag NS-based detection system clearly demonstrated its potential as an on-site, rapid, sensitive, and label-free method for the detection of target molecules.

EXPERIMENTAL SECTION

Materials. Tetraethyhlorthosilicate (TEOS), 3-mercaptopropyl trimethoxysilane (MPTS), ethylene glycol (EG), poly-(vinylpyrrolidone) (PVP, $M_w \approx 40\,000$), silver nitrate ($AgNO_3$, 99.99+%), and octylamine (OA) were purchased from Sigma-Aldrich (St. Louis, MO, USA) and used without further purification. Thiram was purchased by Alfa Aesar (Ward Hill, MA, USA). Ammonium hydroxide (NH_4OH, 27%) and ethanol (98%) were provided by Daejung (Busan, Korea). Deionized (DI) water was used for all experiments. The apples were purchased from a local market.

Synthesis of Ag-Nanoshells (Ag NSs). Tetraethylorthosilicate (TEOS, 1.6 mL) was dissolved in 40 mL of absolute ethanol, and a 3 mL portion of ammonium hydroxide (27%) was added to the ethanol mixture. The resulting mixture was then vigorously stirred using a magnetic bar for 20 h at 25 °C. Next, the synthesized silica nanoparticles (Silica NPs) were centrifuged and washed with ethanol several times to remove excess reagents. The resulting silica NPs were then functionalized with a thiol group.The silica NPs (300 mg) were then dispersed in 6 mL of ethanol containing 300 μL of MPTS and 60 μL of aqueous ammonium hydroxide (27%). The mixture was stirred for 12 h at 25 °C, and the resulting MPTS-treated silica NPs were centrifuged and washed several times with ethanol. Various amounts of MPTS-treated Si NPs were dispersed in 25 mL aliquots of ethylene glycol containing 5 mg of PVP, after which 25 mL of an $AgNO_3$ solution (to a final $AgNO_3$ concentration of 3.5 mM) was added to the silica dispersion and thoroughly mixed. A 41.3 μL aliquot of octylamine (5 mM) was then rapidly added into the silica dispersion, and the resulting mixture was stirred for varying amounts of time ranging from 10 s to 1 h at 25 °C. Finally, the Ag-nanoshells (Ag NSs) were centrifuged and washed with ethanol several times for purification.

Thiram Detection in Ethanol. Thiram was prepared at various concentrations in ethanol. After dilution to the desired concentrations, 100 μL of each thiram solution was added into a 900 μL of a solution of the Ag NSs (1 mg/mL). The mixture was gently shaken for 10 min

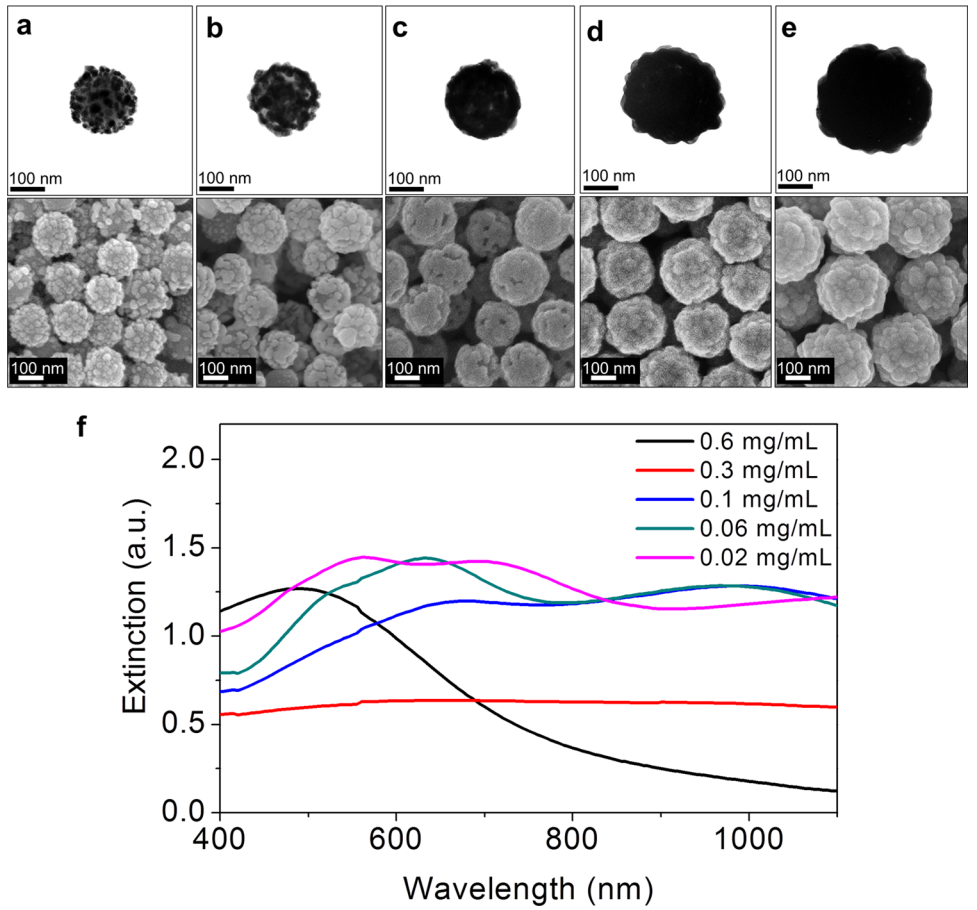

Figure 2. Effect of silica NPs concentrations on the formation of Ag-Nanoshells (Ag NSs). (a) TEM (upper panel) and FE-SEM (lower panel) images of Ag NSs prepared with 0.6 mg/mL of silica NPs, (b) 0.3 mg/mL of silica NPs, (c) 0.1 mg/mL of silica NPs, (d) 0.06 mg/mL of silica NPs, and (e) 0.02 mg/mL of silica NPs. (f) UV/vis extinction spectra of Ag-NSs prepared at various concentrations of silica NPs. The concentrations of $AgNO_3$ and octylamine were 3.5 and 5 mM, respectively. Ag NSs completely formed on the silica surface as the concentration of silica NPs became lower than 0.06 mg/mL.

and concentrated to 10 mg/mL. The thiram-containing Ag NSs solution (~0.5 μL) was dropped on a glass substrate and dried under ambient conditions. The Raman spectra of thiram were measured from the Ag NSs using a 785 nm laser with 60 mW power.

Thiram Detection on Apple Peels. Aliquots (0.5 μL) of thiram solutions at different concentrations were dropped onto apple peels and dried completely. A 0.5 μL aliquot of Ag NSs solution (10 mg/mL) was then dropped onto the thiram-containing apple peels. After evaporating the solvent, the Raman spectra were obtained from apple peels using a 785 nm laser with 30 mW power for 5 s.

Instruments. The absorption spectra of the Ag NSs were measured using a UV spectrometer (Optizen 2120UV, Mecasys). The morphology and size of the Ag NSs were characterized using a field emission scanning electron microscope (FE-SEM, JSM-6701F, JEOL) and a transmission electron microscope (TEM, LIBRA 120, Carl Zeiss). Ethylene glycol/silver ion complex was analyzed by Quattro triple quadrupole tandem mann spectrometer (Waters/Micromass), FT-IR spectroscopy instrument (Nicolet 6700, Thermo Scientific). The SERS spectra were obtained using a portable-Raman system (B&W TEK, i-Raman) equipped with a diode laser emitting at 785 nm.

RESULTS AND DISCUSSION

Systematic Study of the Synthesis of Ag Nanoshells (Ag NSs). For the single-step synthesis of Ag NSs without predeposition of seed metals, silica nanoparticles (Silica NPs) (150 nm in diameter) were synthesized by the Stöber method,[52] and subsequently modified with 3-mercaptopropyltrimethoxysilane (MPTS) to impart high affinity to Ag NPs.[53] The thiol-functionalized silica NPs were then mixed with $AgNO_3$, octylamine as a mild reducing agent, and poly(vinylpyrrolidone) (PVP) as a surface passivation agent in ethylene glycol at room temperature for the synthesis of Ag NSs (Figure 1). During the reaction, the concentrations of $AgNO_3$, octylamine, and silica NPs, as well as the reaction time were varied to identify the optimal conditions for the formation of uniform and complete Ag shells onto a core. Specifically, the effect of the concentration of $AgNO_3$ and octylamine on the formation of Ag NSs was first investigated at a fixed reaction time of 1 h and the silica NPs concentration of 1 mg/mL. As the concentration of both $AgNO_3$ and octylamine increased from 1 to 5 mM, a larger number of Ag NPs were formed on the silica NPs, and their size also increased (Figure S1, Supporting Information). At concentrations of $AgNO_3$ and octylamine higher than 3 mM, Ag NPs were also produced in the solution, which resulted in large aggregates of Ag NPs. The effect of octylamine concentrations was further explored at a predetermined concentration of $AgNO_3$ (3 mM). As the concentration of octylamine increased from 1 to 5 mM, larger sizes of Ag NPs were introduced more densely only on the surface of the silica NPs without formation in the solution (Figure S1, Supporting Information). However, at a much higher concentration of octylamine (10 mM), the Ag NPs formed irregularly on each core particle, as shown in

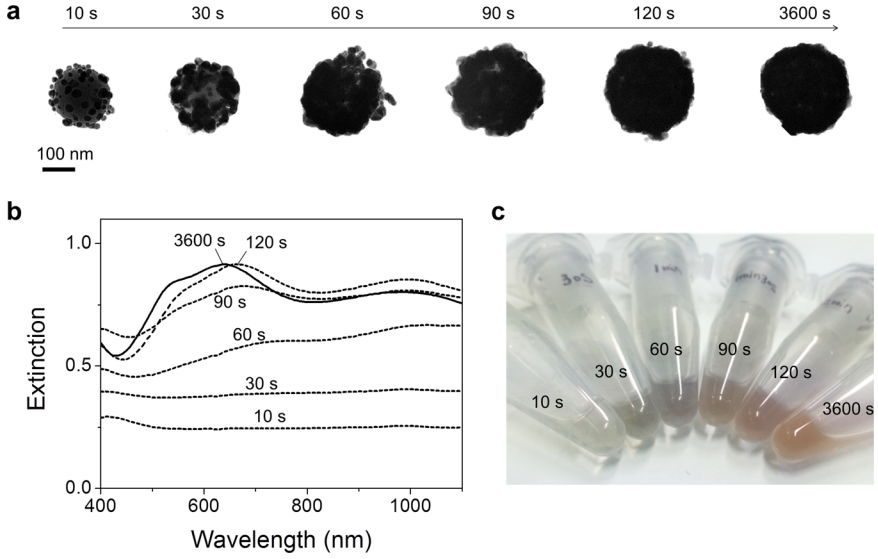

Figure 3. Kinetics of the formation of Ag-nanoshells (Ag NSs). (a) TEM images and (b) UV/vis extinction spectra of growing Ag NSs as a function of reaction time ranging from 10, 30, 60, 90, 120, and 3600 s. (c) Photograph of Ag NSs solution at various reaction times, showing the change in color.

Supporting Information Figure S1. With further optimization, the optimal concentrations of $AgNO_3$ (3.5 mM) and octylamine (5 mM) were identified, and were used for further investigation of the other variables in the formation of Ag NSs.

Having identified the optimal concentrations of $AgNO_3$ and octylamine, the influence of reaction time on the formation of Ag NSs was then examined. Reaction times were varied from 1 to 6 h at room temperature. As shown in Supporting Information Figure S2, the density of Ag NPs on the surface of the silica NPs increased gradually as the reaction time increased. Some portions of the particles were fully covered by the Ag shells in 6 h. However, the resulting particles exhibited a large distribution in the Ag shell coverage and a nonuniform formation of the Ag shell on the core particles because of Ostwald ripening (Figure S2, Supporting Information). Although it did not result in complete formation of Ag NSs, a reaction time of 1 h was determined to be optimal to obtain a homogeneous formation of Ag NPs only on the surface of silica NPs.

Finally, we explored the effect of the concentrations of silica NPs. The concentration of silica NPs was varied from 0.6 to 0.02 mg/mL with the optimized concentration of $AgNO_3$ (3.5 mM) and octylamine (5 mM), and the reaction time of 1 h at room temperature. Figure 2a–e shows TEM and SEM images of the particles synthesized at each concentration of silica NPs (0.6, 0.3, 0.1, 0.06, and 0.02 mg/mL, respectively). When 0.6 mg/mL of silica NPs was added into the $AgNO_3$ solution, a large amount of dense Ag NPs were created on the silica surface (Figure 2a). The coverage of the Ag NPs on the cores steadily increased with decreasing concentration of the silica NPs, which led to the formation of a network-like shell structure (Figure 2b and c). As the concentration of silica NPs reached 0.06 mg/mL, a complete layer of Ag shells, fully covering the surface of the core particles, was obtained. The thickness of the Ag shells on the silica cores was 40 nm (Figure 2d), which could be further increased up to 70 nm by using much lower concentrations of Si NPs (0.02 mg/mL, Figure 2e). It is noteworthy that the morphology of the Ag NSs exhibited a bumpy structure, which is beneficial in creating "hot spots" that induce a strong EM field enhancement compared with smooth surfaces.[54] Furthermore, the SERS signals for the molecules of interest could be considerably enhanced on the bumpy surface of Ag NSs. In addition to electron microscopy, the formation of Ag NSs was also confirmed by absorption spectroscopy. As shown in Figure 2f, the particles obtained at a silica NP concentration of 0.6 mg/mL showed a single plasmon absorption band between 400 and 500 nm (black line), which corresponded to the structure with separated Ag NPs on the surface. As Ag NPs coalesced into a network-like structure at lower concentrations of silica NPs, the distinct absorption band disappeared, but the broadband and flat absorption in a broad range of wavelength (400–1400 nm) was observed (Figure 2f and Supporting Information Figure S3, red line).[27] This abnormal absorption may be attributed to the diversity in the size and the shape of Ag clusters, which gives rise to the continuous spectrum of resonant dipole and multipole modes.[55,56] With respect to the silica NP concentration of 0.1 mg/mL, the plasmon absorption spectra of the particles changed to broad bands that spread from the visible to the NIR region (blue, green and pink lines), indicating that a complete layer of Ag shell was formed on the silica NPs. Furthermore, the plasmon absorption of the Ag NSs was shifted toward shorter wavelengths as the thickness of the Ag shells increased, which was attributed to coupling between the inner and outer surfaces.[57] As the Ag shell thickness increased beyond the dipole limit, shoulder peaks appearing at ~550 nm were observed again due to multipolar plasmon resonance.[58]

According to the results of our systematic experiments, Ag NSs with uniform, complete shells were successfully synthesized in a single step at room temperature, without requiring the deposition of seed metals. Our results also confirmed that the concentration of silica NPs was the most critical factor for the complete formation of Ag NSs.

Kinetics and Mechanism for Ag NSs Formation. We next investigated the kinetics for the formation of Ag NSs under the optimal conditions (3.5 mM of $AgNO_3$, 5 mM of octylamine, and 0.06 mg/mL of silica NPs). The progress of the Ag NS formation was monitored by TEM and with an

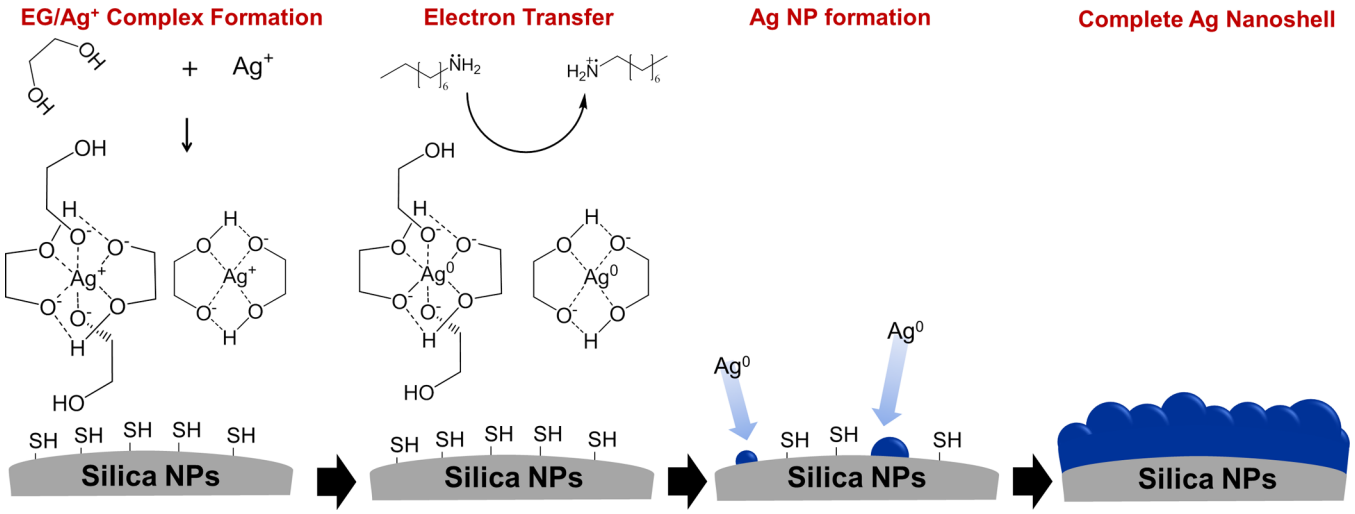

Figure 4. Proposed reaction mechanism for fast single-step formation of Ag NSs.

absorption spectrophotometer at each time interval (10, 30, 60, 90, 120, and 3600 s) as shown in Figure 3. TEM images of the particles suggested that the reduction of Ag^+ ions and the nucleation of Ag^0 took place almost immediately, occurring within 10 s at 25 °C without any strong reductant (Figure 3a). This was abnormally fast compared to the conventional synthetic protocols for Ag NSs. Small Ag NPs on the surface of the silica NPs continued to grow as a function of the reaction time, and the Ag NSs were completely formed after 120 s. As the reaction time further increased beyond 120 s, no remarkable change in the size and morphology of the Ag NSs were observed. Based on these observations, we concluded that a uniform and complete Ag shell on the silica NPs was created in a single step within 120 s at 25 °C without the use of any strong reductant. To the best of our knowledge, this is the first report of such quick formation of Ag NSs within 120 s at 25 °C without the deposition of seed metals. The rapid formation of Ag NSs was confirmed by the plasmon absorption spectra (Figure 3b), which showed the appearance of distinct extinction bands at around 670 and 1000 nm at 120 s, which were identical to those of the Ag NSs obtained after 60 min. This plasmon absorption clearly corresponded to the structure of Ag NSs as shown in the TEM images (Figure 3a). As can be seen in Figure 3c, the color of the Ag NS dispersions changed immediately from light gray to brownish-red within 120 s, indicating the rapid formation of Ag NSs.

Next, the mechanism for the rapid growth of Ag NSs at room temperature in absence of a strong reducing agent was examined. We were most interested in determining the mechanism responsible for the reduction of Ag^+ ions to Ag^0 under such mild conditions. To this end, a reaction without octylamine was conducted in ethylene glycol (EG) at 25 °C for 60 min. As shown in Supporting Information Figure S3a, no Ag NP was obtained on the surface of the silica NPs, indicating that EG was incapable of reducing Ag^+ ions at room temperature. In the conventional polyol method, it was reported that EG plays a role as a reducing agent as well as a solvent, and that the reduction process generally occurs at a high temperature (above 150 °C).[59,60] However, this was not the case for the rapid growth of Ag NSs at room temperature. Rather, our results suggested that octylamine might be responsible for the reduction of Ag^+ ions to Ag^0 to initiate the nucleation and growth of the Ag shells. The effect of the solvent (EG) on the rapid growth of Ag NSs was further investigated by performing the reaction in the presence of octylamine, but with the use of other solvents including ethanol, ethylene glycol monoethyl ether and ethylene glycol dimethyl ether. As shown in Supporting Information Figure S3b, no Ag NP was formed on the surface of the silica NPs in ethanol. In ethylene glycol monoethyl ether, only slight introduction of Ag NPs on the silica NPs was observed (Supporting Information Figure S3c). In ethylene glycol dimethyl ether, a large number of Ag NPs were created on the surface of the silica NPs, though the solubility of $AgNO_3$ was poor (Supporting Information Figure S3d). Taken together, these results indicated that EG, a symmetric diol, plays another important role in the fast formation of Ag NSs at room temperature, instead of directly reducing the Ag^+ ions. To further examine the role of EG on the rapid growth of Ag NSs, the reduction potential of Ag^+ ion in both EG and ethanol were measured using cyclic voltammetry (CV). As shown in Supporting Information Figure S4, the reduction potential of the Ag^+ ion increased significantly to a more positive value in EG compared to in ethanol. The increase in the reduction potential of Ag^+ ion in EG seems to allow the facile reduction of Ag^+ by a mild reducing agent (octylamine) even at room temperature. It has been reported that EG can produce a stable complex with metal ions via internal hydrogen bonding.[61] Thus, we speculated that the stable complex of Ag^+ ions with EG could induce a large increase in their reduction potential, and confirmed the formation of an EG/Ag+ ion complex during the course of Ag NS formation using FT-IR and mass spectrometry (Supporting Information Figure S5). The proposed mechanism for the rapid formation of Ag NSs is shown in Figure 4. Specifically, we proposed that Ag^+ ions first form a stable complex with EG, resulting in an increased reduction potential. Octylamine then reduces Ag^+ ions to Ag^0 via single electron transfer from the lone-pair electrons in nitrogen to the ions, which leads to the generation of a radical cation that is subsequently converted to imine and nitrile groups through radical disproportionation.[62]

Label-Free Thiram Detection by SERS with Ag NSs. The Ag NSs produced were applied as SERS-active nanoprobes for the label-free detection of thiram using SERS spectroscopy. Since Ag NSs have a bumpy surface that can induce a strong EM field for SERS enhancement, they are suitable for the

sensitive detection of thiram. As shown in Figure 5a, thiram has a disulfide residue with a high affinity for Ag surfaces, and can

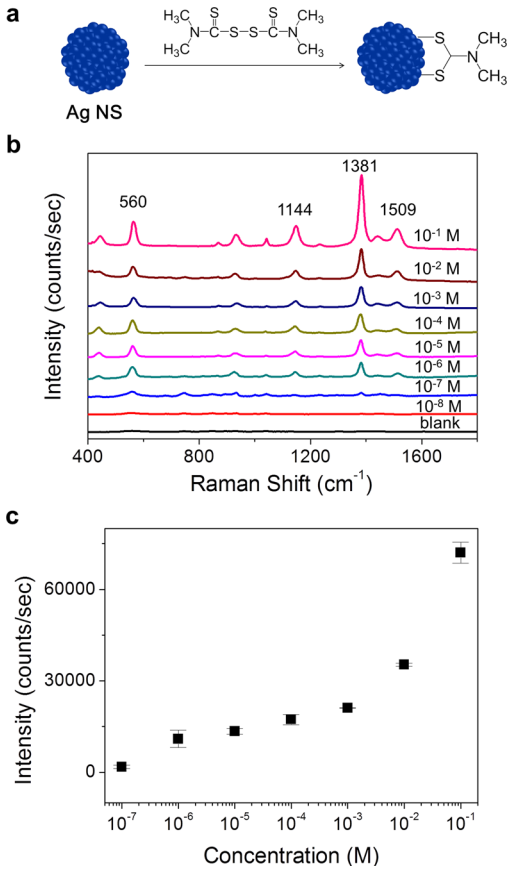

Figure 5. SERS detection of thiram on Ag NSs. (a) Schematic illustration of thiram adsorption on Ag NS surfaces for SERS detection. (b) SERS spectra of thiram at various concentrations. (c) SERS intensity of thiram at 1381 cm^{-1} as a function of thiram concentrations showing a linear correlation. Ag NSs prepared with 0.06 mg/mL of silica NPs were used. SERS spectra were obtained using a 785 nm laser with 60 mW power.

easily approach the Ag NSs through chemisorption. For thiram detection, Ag NSs were first added into an ethanol solution containing thiram at various concentrations. The resulting mixture was gently shaken for 10 min. The Raman signals of thiram were recorded using a portable Raman system after dropping and air-drying the solution (~0.5 μL) ontol a glass substrate. Figure 5b shows the strong SERS signals of thiram at each concentration (10^{-1} to 10^{-8} M), confirming that the Ag NSs were an active SERS substrate suitable for large enhancement of the signal. Specifically, the intensities of the Raman bands at 560, 1144, 1381, and 1509 cm^{-1} increased with increasing concentrations of thiram. The band at 1381 cm^{-1} is associated with the symmetric CH_3 deformation mode weakly coupled to the CN stretching mode. The band at 1509 cm^{-1} is attributed to the CN stretching mode, and the one at 1144 cm^{-1} is attributed to the rocking CH_3 mode weakly coupled to the CN stretching mode. The bands at 560 cm^{-1} is associated with the SS stretching mode.[39,43] Figure 5c shows the linear correlation between the peak intensity at 1381 cm^{-1} and the thiram concentrations. In support of the sensitive nature of Ag NS-based label-free detection, we calculated the limit of detection (LOD) of Ag NSs system for thiram detection based on the standard deviation of the response (SD) and the slope of the calibration curve (S) at levels approximating the LOD according to the formula: LOD = 3.3(SD/S). We found that its LOD was 6 μM. Furthermore, we conducted control experiment to demonstrate the sensitivity of Ag NS-based SERS detection of thiram using conventional HPLC system. In HPLC system, the LOD was 15.7 μM, which is higher than Ag NS-based SERS detection. Therefore, Ag NS-based SERS substrate could allow more sensitive detection of thiram compared to conventional analytical method.

The large enhancement of the Raman signal of thiram on the bumpy Ag NSs demonstrated their potential for the practical SERS-based on-site detection of thiram on fruit peels. To validate this concept, thiram adsorbed on the surface of apple peels was detected and quantified using the Ag NS-based label-free detection method.[37] As shown in Figure 6a, apple peels

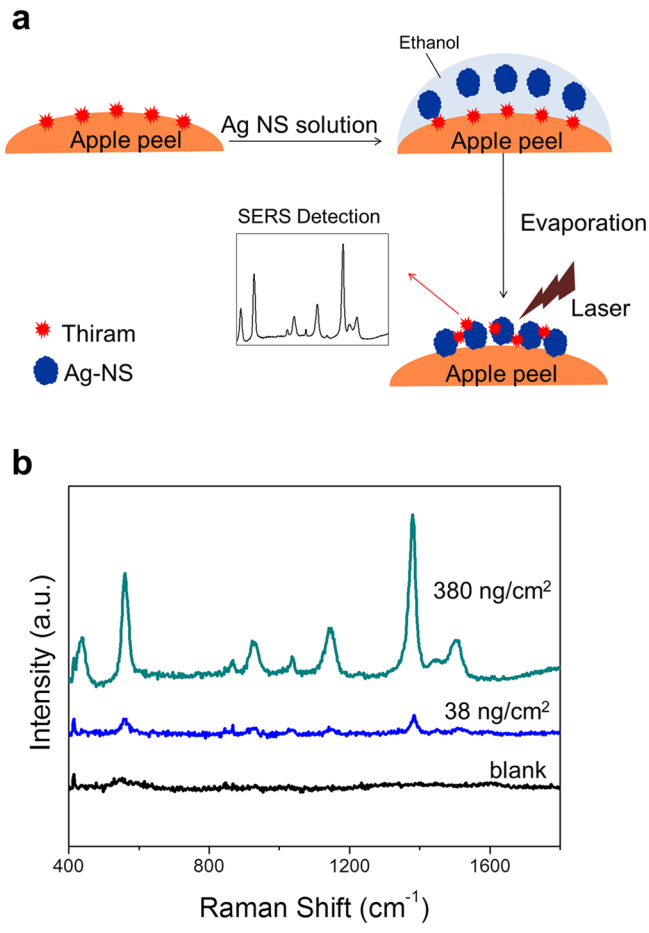

Figure 6. On-site detection of thiram on an apple peels using Ag NSs. (a) Schematic illustration of the on-site detection of residual thiram on an apple peels based on SERS. (b) SERS spectra of residual thiram on an apple peels after addition of Ag NSs (10 mg/mL). SERS spectra were obtained using a 785 nm laser with 30 mW power for 5 s.

were cut into squares of 1 cm^2, and 0.5 μL of thiram solutions of different concentrations was dropped onto the surface. After evaporation of the solvent, the Ag NS solution (~0.5 μL, 10 mg/mL in ethanol) was added to the peel and allowed to interact with thiram. The SERS spectra were then obtained using the portable Raman system after evaporating the solvent (Figure 6a). Figure 6b shows the SERS spectra of the thiram residues collected from the apple peel. The characteristic bands

dx.doi.org/10.1021/am502435x | ACS Appl. Mater. Interfaces 2014, 6, 12541−12549

of thiram appeared strongly, and their intensity increased with increasing concentrations of thiram on the peel. This strong enhancement of the Raman signals for thiram was due to the hot spots created by the aggregated Ag NSs bearing thiram during the evaporation of the solvent. According to these results, the Ag NS-based label-free approach was able to sensitively detect thiram at a level of 38 ng/cm^2, which is much lower than the maximum permissible level of ~2 μg/cm^2 for apple peels.[37] Thus, our results clearly demonstrate the potential of bumpy Ag NSs for use in the on-site detection of residual pesticides in a label-free manner.

CONCLUSIONS

Ag NSs were rapidly synthesized in a single-step at room temperature, without the predeposition of seed metals on a dielectric core. The mechanism for the abnormally rapid kinetics in the formation of Ag NSs was explored, and it was found that the favorable electron transfer from octylamine to Ag^+ ions was likely due to a large increase in the reduction potential of the stable complex of Ag^+ ions with ethylene glycol. This new approach enables control of both the shell thickness of Ag NSs and their optical properties. The Ag NSs were successfully applied for label-free detection of thiram on apple peels, thereby demonstrating their potential for use as a SERS-based on-site detection method for various pesticides.

ASSOCIATED CONTENT

Supporting Information

TEM images of the Ag NPs-embedded silica NPs at various concentrations of $AgNO_3$ and octylamine, TEM images of Ag NSs prepared at various reaction time, TEM images showing the effect of base and solvent on the formation of Ag NSs, cyclic voltammogram of $AgNO_3$ in ethylene glycol and ethanol, FT-IR and MS spectra of ethylene glycol–Ag^+ ion mixture, and HPLC spectra of various concentrations of thiram. This material is available free of charge via the Internet at http://pubs.acs.org

AUTHOR INFORMATION

Corresponding Authors

*E-mail: kjh75@hanyang.ac.kr.

*E-mail: yslee@snu.ac.kr. Phone: +82-2-880-7073. Fax: +82-2-876-9625.

Present Address

#School of Electrical Engineering and Computer Science, Seoul National University, Seoul, Republic of Korea.

Author Contributions

J.-K.Y., H.K., J.-H.K., and Y.-S.L. created the idea and designed all experiments. In addition, these authors wrote the manuscript. J.-K.Y., H.K., H.L., and A.J. synthesized the Ag nanoshells at various reaction conditions and characterized the as-prepared particles. J.-K.Y., H.K., S.J., S.-J.J., and H.-I.K. carried out analytical experiments. H.-Y.L., D.-H.J., J.-H.K., and Y.-S.L. supervised the research. All authors gave comments on the experimental results, as well as on the manuscript.

Notes

The authors declare no competing financial interest.

ACKNOWLEDGMENTS

This research was supported by grants from the Pioneer Research Center Program (2013-006163), the Science Research Program (2008-0061860), the Basic Science Research Program (2012-R1A1A1012516) through the National Research Foundation of the Korean government (NRF) funded by the Ministry of Science, ICT & Future planning, and the Bio & Medical Technology Development Program (2013-035616) of NRF funded by the Ministry of Education.

REFERENCES

(1) Chen, C.-W.; Serizawa, T.; Akashi, M. Preparation of Platinum Colloids on Polystyrene Nanospheres and Their Catalytic Properties in Hydrogenation. *Chem. Mater.* **1999**, *11*, 1381–1389.

(2) Ochsenkühn, M. A.; Jess, P. R.; Stoquert, H.; Dholakia, K.; Campbell, C. J. Nanoshells for Surface-Enhanced Raman Spectroscopy in Eukaryotic Cells: Cellular Response and Sensor Development. *ACS Nano* **2009**, *3*, 3613–3621.

(3) Sershen, S.; Westcott, S.; Halas, N.; West, J. Temperature-Sensitive Polymer–Nanoshell Composites for Photothermally Modulated Drug Delivery. *J. Biomed. Mater. Res.* **2000**, *51*, 293–298.

(4) Hirsch, L. R.; Stafford, R.; Bankson, J.; Sershen, S.; Rivera, B.; Price, R.; Hazle, J.; Halas, N.; West, J. Nanoshell-Mediated near-Infrared Thermal Therapy of Tumors under Magnetic Resonance Guidance. *Proc. Natl. Acad. Sci. U.S.A.* **2003**, *100*, 13549–13554.

(5) Kundu, J.; Le, F.; Nordlander, P.; Halas, N. J. Surface Enhanced Infrared Absorption (SEIRA) Spectroscopy on Nanoshell Aggregate Substrates. *Chem. Phys. Lett.* **2008**, *452*, 115–119.

(6) Jackson, J. B.; Halas, N. J. Surface-Enhanced Raman Scattering on Tunable Plasmonic Nanoparticle Substrates. *Proc. Natl. Acad. Sci. U.S.A.* **2004**, *101*, 17930–17935.

(7) Prodan, E.; Nordlander, P.; Halas, N. Electronic Structure and Optical Properties of Gold Nanoshells. *Nano Lett.* **2003**, *3*, 1411–1415.

(8) Oldenburg, S.; Averitt, R.; Westcott, S.; Halas, N. Nanoengineering of Optical Resonances. *Chem. Phys. Lett.* **1998**, *288*, 243–247.

(9) Jiang, Z.-j.; Liu, C.-y. Seed-Mediated Growth Technique for the Preparation of a Silver Nanoshell on a Silica Sphere. *J. Phys. Chem. B* **2003**, *107*, 12411–12415.

(10) Halas, N. Playing with Plasmons: Tuning the Optical Resonant Properties of Metallic Nanoshells. *MRS Bull.* **2005**, *30*, 362–367.

(11) Jain, P. K.; Lee, K. S.; El-Sayed, I. H.; El-Sayed, M. A. Calculated Absorption and Scattering Properties of Gold Nanoparticles of Different Size, Shape, and Composition: Applications in Biological Imaging and Biomedicine. *J. Phys. Chem. B* **2006**, *110*, 7238–7248.

(12) Jackson, J.; Halas, N. Silver Nanoshells: Variations in Morphologies and Optical Properties. *J. Phys. Chem. B* **2001**, *105*, 2743–2746.

(13) Kreibig, U.; Vollmer, M. *Optical Properties of Metal Clusters*; Springer: Berlin, 1995.

(14) Kneipp, K.; Dasari, R. R.; Wang, Y. Near-Infrared Surface-Enhanced Raman Scattering (Nir SERS) on Colloidal Silver and Gold. *Appl. Spectrosc.* **1994**, *48*, 951–955.

(15) Kneipp, K.; Kneipp, H.; Kneipp, J. Surface-Enhanced Raman Scattering in Local Optical Fields of Silver and Gold Nanoaggregates from Single-Molecule Raman Spectroscopy to Ultrasensitive Probing in Live Cells. *Acc. Chem. Res.* **2006**, *39*, 443–450.

(16) Liu, T.; Li, D.; Yang, D.; Jiang, M. An Improved Seed-Mediated Growth Method to Coat Complete Silver Shells onto Silica Spheres for Surface-Enhanced Raman Scattering. *Colloids Surf., A* **2011**, *387*, 17–22.

(17) Choma, J.; Dziura, A.; Jamioła, D.; Nyga, P.; Jaroniec, M. Preparation and Properties of Silica–Gold Core–Shell Particles. *Colloids Surf., A* **2011**, *373*, 167–171.

(18) Kobayashi, Y.; Salgueirino-Maceira, V.; Liz-Marzan, L. M. Deposition of Silver Nanoparticles on Silica Spheres by Pretreatment Steps in Electroless Plating. *Chem. Mater.* **2001**, *13*, 1630–1633.

(19) Dokoutchaev, A.; James, J. T.; Koene, S. C.; Pathak, S.; Prakash, G. S.; Thompson, M. E. Colloidal Metal Deposition onto Functionalized Polystyrene Microspheres. *Chem. Mater.* **1999**, *11*, 2389–2399.

(20) Caruso, F.; Spasova, M.; Salgueiriño-Maceira, V.; Liz-Marzán, L. Multilayer Assemblies of Silica-Encapsulated Gold Nanoparticles on Decomposable Colloid Templates. *Adv. Mater.* **2001**, *13*, 1090−1094.
(21) Dong, A.; Wang, Y.; Tang, Y.; Ren, N.; Yang, W.; Gao, Z. Fabrication of Compact Silver Nanoshells on Polystyrene Spheres through Electrostatic Attraction. *Chem. Commun.* **2002**, 350−351.
(22) Cassagneau, T.; Caruso, F. Contiguous Silver Nanoparticle Coatings on Dielectric Spheres. *Adv. Mater.* **2002**, *14*, 732.
(23) Schueler, P. A.; Ives, J. T.; DeLaCroix, F.; Lacy, W. B.; Becker, P. A.; Li, J.; Caldwell, K. D.; Drake, B.; Harris, J. M. Physical Structure, Optical Resonance, and Surface-Enhanced Raman Scattering of Silver-Island Films on Suspended Polymer Latex Particles. *Anal. Chem.* **1993**, *65*, 3177−3186.
(24) Pol, V. G.; Srivastava, D.; Palchik, O.; Palchik, V.; Slifkin, M.; Weiss, A.; Gedanken, A. Sonochemical Deposition of Silver Nanoparticles on Silica Spheres. *Langmuir* **2002**, *18*, 3352−3357.
(25) Kang, H.; Kang, T.; Kim, S.; Kim, J.-H.; Jun, B.-H.; Chae, J.; Park, J.; Jeong, D.-H.; Lee, Y.-S. Base Effects on Fabrication of Silver Nanoparticles Embedded Silica Nanocomposite for Surface-Enhanced Raman Scattering (Sers). *J. Nanosci. Nanotechnol.* **2011**, *11*, 579−583.
(26) Wang, W.; Asher, S. A. Photochemical Incorporation of Silver Quantum Dots in Monodisperse Silica Colloids for Photonic Crystal Applications. *J. Am. Chem. Soc.* **2001**, *123*, 12528−12535.
(27) Kim, K.; Kim, H. S.; Park, H. K. Facile Method to Prepare Surface-Enhanced-Raman-Scattering-Active Ag Nanostructures on Silica Spheres. *Langmuir* **2006**, *22*, 8083−8088.
(28) Lee, J.-M.; Kim, D.-W.; Jun, Y.-D.; Oh, S.-G. Preparation of Silica−Silver Heterogeneous Nanocomposite Particles by One-Pot Preparation Strategy Using Polyol Process: Size-Controlled Immobilization of Silver Nanoparticles. *Mater. Res. Bull.* **2006**, *41*, 1407−1416.
(29) Tuval, T.; Gedanken, A. A Microwave-Assisted Polyol Method for the Deposition of Silver Nanoparticles on Silica Spheres. *Nanotechnology* **2007**, *18*, 255601.
(30) Kneipp, J.; Kneipp, H.; Kneipp, K. SERS—A Single-Molecule and Nanoscale Tool for Bioanalytics. *Chem. Soc. Rev.* **2008**, *37*, 1052−1060.
(31) Haynes, C. L.; MacFarland, A. D.; Van Duyne, R. P. Surface-Enhanced Raman Spectroscopy. *Anal. Chem.* **2005**, 338A−346A.
(32) Alvarez-Puebla, R. A.; Liz-Marzan, L. M. Traps and Cages for Universal SERS Detection. *Chem. Soc. Rev.* **2012**, *41*, 43−51.
(33) Schlücker, S. Surface-Enhanced Raman Spectroscopy: Concepts and Chemical Applications. *Angew. Chem., Int. Ed.* **2014**, *53*, 4756−4795.
(34) Cao, Y. C.; Jin, R.; Mirkin, C. A. Nanoparticles with Raman Spectroscopic Fingerprints for DNA and RNA Detection. *Science* **2002**, *297*, 1536−1540.
(35) Zhang, X.; Young, M. A.; Lyandres, O.; Van Duyne, R. P. Rapid Detection of an Anthrax Biomarker by Surface-Enhanced Raman Spectroscopy. *J. Am. Chem. Soc.* **2005**, *127*, 4484−4489.
(36) Han, X. X.; Huang, G. G.; Zhao, B.; Ozaki, Y. Label-Free Highly Sensitive Detection of Proteins in Aqueous Solutions Using Surface-Enhanced Raman Scattering. *Anal. Chem.* **2009**, *81*, 3329−3333.
(37) Li, X.; Chen, G.; Yang, L.; Jin, Z.; Liu, J. Multifunctional Au-Coated TiO_2 Nanotube Arrays as Recyclable SERS Substrates for Multifold Organic Pollutants Detection. *Adv. Funct. Mater.* **2010**, *20*, 2815−2824.
(38) Valentine, W. M.; Amarnath, V.; Amarnath, K.; Rimmele, F.; Graham, D. G. Carbon Disulfide Mediated Protein Crosslinking by N, N-Diethyldithiocarbamate. *Chem. Res. Toxicol.* **1995**, *8*, 96−102.
(39) Saute, B.; Premasiri, R.; Ziegler, L.; Narayanan, R. Gold Nanorods as Surface Enhanced Raman Spectroscopy Substrates for Sensitive and Selective Detection of Ultra-Low Levels of Dithiocarbamate Pesticides. *Analyst* **2012**, *137*, 5082−5087.
(40) Zhang, L.; Jiang, C.; Zhang, Z. Graphene Oxide Embedded Sandwich Nanostructures for Enhanced Raman Readout and Their Applications in Pesticides Monitoring. *Nanoscale* **2013**, *5*, 3773−3779.
(41) Liu, B.; Han, G.; Zhang, Z.; Liu, R.; Jiang, C.; Wang, S.; Han, M. Y. Shell Thickness-Dependent Raman Enhancement for Rapid Identification and Detection of Pesticide Residues at Fruit Peels. *Anal. Chem.* **2012**, *84*, 255−261.
(42) Yuan, C.; Liu, R.; Wang, S.; Han, G.; Han, M.-Y.; Jiang, C.; Zhang, Z. Single Clusters of Self-Assembled Silver Nanoparticles for Surface-Enhanced Raman Scattering Sensing of a Dithiocarbamate Fungicide. *J. Mater. Chem.* **2011**, *21*, 16264−16270.
(43) Kang, J. S.; Hwang, S. Y.; Lee, C. J.; Lee, M. S. SERS of Dithiocarbamate Pesticides Adsorbed on Silver Surface; Thiram. *Bull. Korean Chem. Soc.* **2002**, *23*, 1604−1610.
(44) Sharma, V. K.; Aulakh, J.; Malik, A. K. Thiram: Degradation, Applications and Analytical Methods. *J. Environ. Monit.* **2003**, *5*, 717−723.
(45) Maini, P.; Boni, R. Gas Chromatographic Determination of Dithiocarbamate Fungicides in Workroom Air. *Bull. Environ. Contam. Toxicol.* **1986**, *37*, 931−937.
(46) Ubeda, M. R.; Escribano, M.; Hernandez, L. H. Determination of Thiram by High-Performance Liquid Chromatography with Amperometric Detection in River Water and Fungicide Formulations. *Microchem. J.* **1990**, *41*, 22−28.
(47) Brandšteterová, E.; Lehotay, J.; Liška, O.; Garaj, J.; Zacsik, I. Application of High-Performance Liquid Chromatography in the Trace Analysis of Some Fungicides. *J. Chromatogr. A* **1984**, *286*, 339−345.
(48) Verma, B. C.; Sood, R.; Sidhu, H. A New Colorimetric Method for the Determination of Carbon Disulphide and Its Application to the Analysis of Some Dithiocarbamate Fungicides. *Talanta* **1983**, *30*, 787−788.
(49) Procopio, J. R.; Escribano, M. T. S.; Hernandez, L. H. Determination of Thiram in Water and Soils by Cathodic Stripping Voltammetry Based on Adsorptive Accumulation. *Fresen. Z. Anal. Chem.* **1988**, *331*, 27−29.
(50) Malik, A. K.; Faubel, W. Capillary Electrophoretic Determination of Tetramethylthiuram Disulphide (Thiram). *Anal. Lett.* **2000**, *33*, 2055−2064.
(51) Kang, H.; Yang, J.-K.; Noh, M. S.; Jo, A.; Jeong, S.; Lee, M.; Lee, S.; Chang, H.; Lee, H.; Jeon, S.-J.; Kim, H.-I.; Lee, H.-Y.; Cho, M.-H.; Kim, J.-H.; Jeong, D. H.; Lee, Y.-S. One-Step Synthesis of Silver Nanoshells with Bumps for Highly Sensitive Near-IR SERS Nanoprobes. *J. Mater. Chem. B* **2014**, *2*, 4415−4421.
(52) Stöber, W.; Fink, A.; Bohn, E. Controlled Growth of Monodisperse Silica Spheres in the Micron Size Range. *J. Colloid Interface Sci.* **1968**, *26*, 62−69.
(53) Gui, J. Y.; Stern, D. A.; Frank, D. G.; Lu, F.; Zapien, D. C.; Hubbard, A. T. Adsorption and Surface Structural Chemistry of Thiophenol, Benzyl Mercaptan, and Alkyl Mercaptans. Comparative Studies at Silver (111) and Platinum (111) Electrodes by Means of Auger Spectroscopy, Electron Energy Loss Spectroscopy, Low Energy Electron Diffraction and Electrochemistry. *Langmuir* **1991**, *7*, 955−963.
(54) Moskovits, M. Surface-Enhanced Raman Spectroscopy: A Brief Retrospective. *J. Raman Spectrosc.* **2005**, *36*, 485−496.
(55) Genov, D. A.; Sarychev, A. K.; Shalaev, V. M. Metal-Dielectric Composite Filters with Controlled Spectral Windows of Transparency. *J. Nonlinear Opt. Phys. Mater.* **2003**, *12*, 419−440.
(56) Biswas, A.; Eliers, H.; Hidden Jr, F.; Aktas, O. C.; Kiran, C. V. S. Large Broadband Visible to Infrared Plasmonic Absorption from Ag Nanoparticles with a Fractal Structure Embedded in a Teflon AF Matrix. *Appl. Phys. Lett.* **2006**, *88*, No. 013103.
(57) Prodan, E.; Radloff, C.; Halas, N.; Nordlander, P. A Hybridization Model for the Plasmon Response of Complex Nanostructures. *Science* **2003**, *302*, 419−422.
(58) Oldenburg, S. J.; Jackson, J. B.; Westcott, S. L.; Halas, N. Infrared Extinction Properties of Gold Nanoshells. *Appl. Phys. Lett.* **1999**, *75*, 2897−2899.
(59) Fievet, F.; Lagier, J.; Blin, B.; Beaudoin, B.; Figlarz, M. Homogeneous and Heterogeneous Nucleations in the Polyol Process for the Preparation of Micron and Submicron Size Metal Particles. *Solid State Ionics* **1989**, *32*, 198−205.

(60) Skrabalak, S. E.; Wiley, B. J.; Kim, M.; Formo, E. V.; Xia, Y. On the Polyol Synthesis of Silver Nanostructures: Glycolaldehyde as a Reducing Agent. *Nano Lett.* **2008**, *8*, 2077−2081.
(61) Gorai, S.; Ganguli, D.; Chaudhuri, S. Synthesis of Copper Sulfides of Varying Morphologies and Stoichiometries Controlled by Chelating and Nonchelating Solvents in a Solvothermal Process. *Cryst. Growth Des.* **2005**, *5*, 875−877.
(62) Janovský, I.; Knolle, W.; Naumov, S.; Williams, F. EPR Studies of Amine Radical Cations, Part 1: Thermal and Photoinduced Rearrangements of *N*-Alkylamine Radical Cations to Their Distonic Forms in Low-Temperature Freon Matrices. *Chem.—Eur. J.* **2004**, *10*, 5524−5534.